A pressure drop model for helium flow in CIC Conductors based on porous media analogy

Zhicai Ma, Yuanwen Gao, Email: ywgao@lzu.edu.cn

College of Civil Engineering and Mechanics, Lanzhou University, Lanzhou, Gansu 730000, P.R. China

Presentation ID：Mon-Af-Po1.18-09

MT 26 International Conference on Magnet Technology, Vancouver, Canada | 2019

Introduction

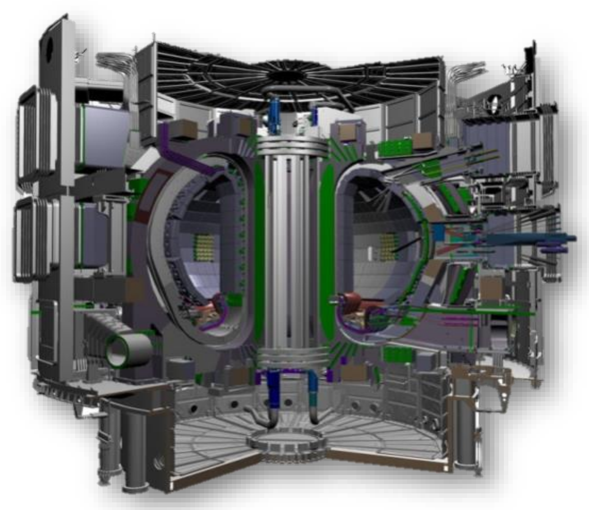

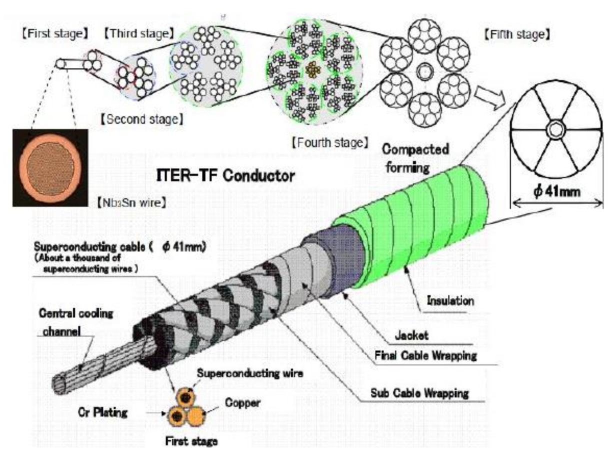

- Cable-in-Conduit Conductors (CICCs) are being developed for use in large superconducting coils, such as tokamaks, stellarators or high energy experimental devices.
- Pressure drop in CICCs cooled by a forced-flow of helium is one of the key parameters for the design of large superconducting magnet systems, which determines the heat removal capability and the thermal stability.
- In order to predict the pressure drop for a given mass flow, an analytical correlation between the mass flow and pressure drop needs to be established.

Theoretical model

The helium flow through channels in CICCs is laminar flow at low Reynolds number and turbulent flow at high Reynolds number. The flow channels are assumed to be a bundle of tortuous capillaries with a series of contracting and expanding sections. The total pressure drop in CICCs is the sum of the pressure drop caused by the viscous energy loss and the local energy.

Pressure drop caused by the viscous energy loss

$$\left.\begin{aligned} q &= \frac{\pi}{128}\frac{\Delta P_1}{L_t}\frac{d^4}{\mu} \\ A &= \pi D_h^2/4 \end{aligned}\right\} \Rightarrow \bar{v}_s = \frac{q}{A} = \frac{D_h^2}{32\mu\tau}\frac{\Delta P_1}{L_0} \quad (d = D_h, L_t = \tau L_0)$$

$$\frac{\Delta P_1}{L_0} = \frac{32\mu\tau}{D_h^2}\bar{v}_s = \frac{32\mu\tau}{D_h^2}\frac{\dot{m}}{\rho_F A_F} = \frac{32\mu^2\tau}{\rho_F D_h^2}\mathrm{Re}.$$

$$\textit{where}\quad \tau = 1/\cos\bar{\theta},\quad \dot{m} = \rho_F A_F \bar{v}_s,\quad \mathrm{Re} = \dot{m} D_h/\mu/A_F$$

Pressure drop caused by the local energy loss

$$\frac{\Delta P_2}{L_0} = \left(\frac{3}{2} - \frac{5}{2\beta^2} + \frac{1}{\beta^4}\right)\frac{\rho_F\tau}{2l}\bar{v}_t^2 = \left(\frac{3}{2} - \frac{5}{2\beta^2} + \frac{1}{\beta^4}\right)\frac{\tau^3 D_h}{2l\varphi^2}\frac{\dot{m}^2}{\rho_F A_F^2}$$

$$= \left(\frac{3}{2} - \frac{5}{2\beta^2} + \frac{1}{\beta^4}\right)\frac{\mu^2\tau^3}{2l\varphi^2\rho_F D_h^2}\mathrm{Re}^2$$

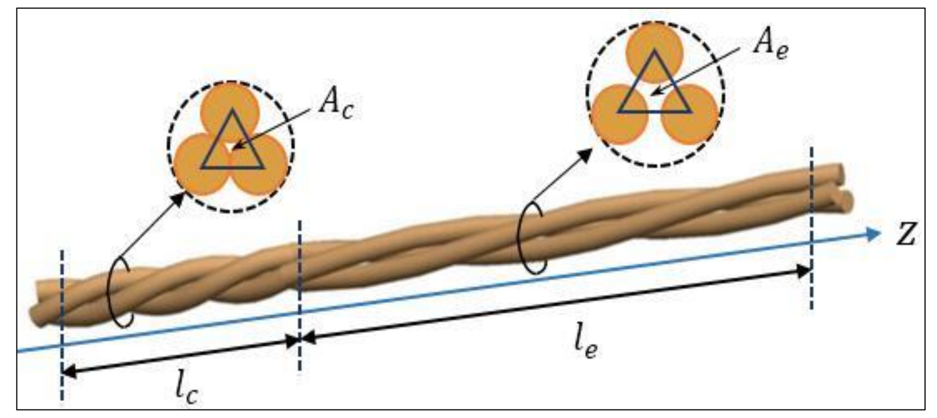

Fig. 1. An initial triplet

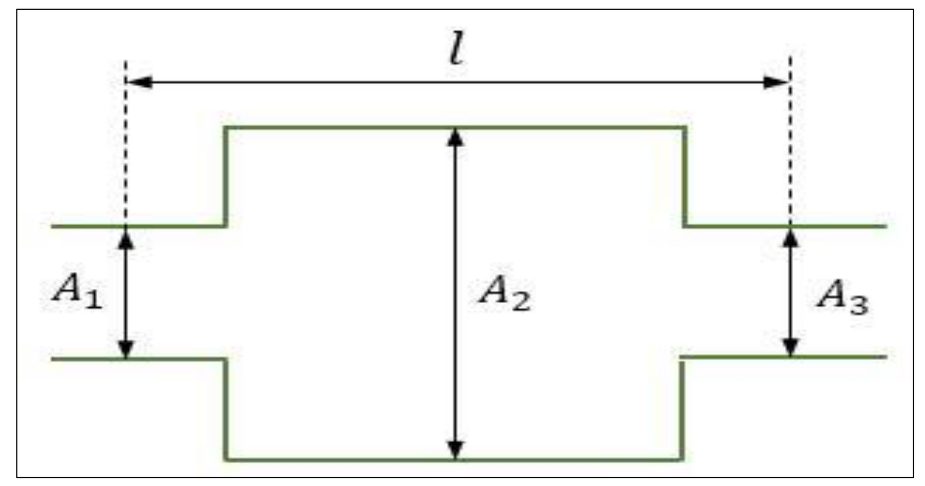

Fig. 2. Pore-throat model

$$\left.\begin{aligned} \bar{v}_t &= \frac{dL_t}{dt} = \tau\frac{dL_0}{dt} = \tau\bar{v}_0 \\ \bar{v}_0 &= \bar{v}_s/\varphi, \\ \bar{v}_t &= \tau\bar{v}_s/\varphi \end{aligned}\right\} \Rightarrow$$

$$l = 100\cdot D_s$$

$$\left.\begin{aligned} \beta &= d_e/d_c = \sqrt{A_c/A_e}, \\ A_c &= \left(\sqrt{3}/4 - \pi/8\right)D_s^2, \\ A_e &= \pi D_s^2\varphi/(1-\varphi)/8 \end{aligned}\right\} \Rightarrow$$

$$\beta = \sqrt{\frac{\pi}{2\sqrt{3}-\pi}\frac{\varphi}{1-\varphi}}$$

Total pressure drop

$$\frac{\Delta P}{L_0} = \frac{\Delta P_1}{L_0} + \frac{\Delta P_2}{L_0} = \frac{32\mu\tau}{D_h^2}\frac{\dot{m}}{\rho_F A_F} + \left(\frac{3}{2} - \frac{5}{2\beta^2} + \frac{1}{\beta^4}\right)\frac{\tau^3}{2l\varphi^2}\frac{\dot{m}^2}{\rho_F A_F^2}$$

$$= \frac{32\mu^2\tau}{\rho_F D_h^3}\mathrm{Re} + \left(\frac{3}{2} - \frac{5}{2\beta^2} + \frac{1}{\beta^4}\right)\frac{\mu^2\tau^3}{2l\varphi^2\rho_F D_h^3}\mathrm{Re}^2$$

$$f = \frac{2D_h\rho_F A_F^2}{\dot{m}^2}\frac{\Delta P}{L_0} = \left(\frac{3}{2} - \frac{5}{2\beta^2} + \frac{1}{\beta^4}\right)\frac{\tau^3 D_h}{l\varphi^2} + \frac{64\tau}{\mathrm{Re}} = a + \frac{b}{\mathrm{Re}}$$

$$\textit{where}\quad a = \left(\frac{3}{2} - \frac{5}{2\beta^2} + \frac{1}{\beta^4}\right)\frac{\tau^3 D_h}{l\varphi^2},\ b = 64\tau.$$

Results and Discussion

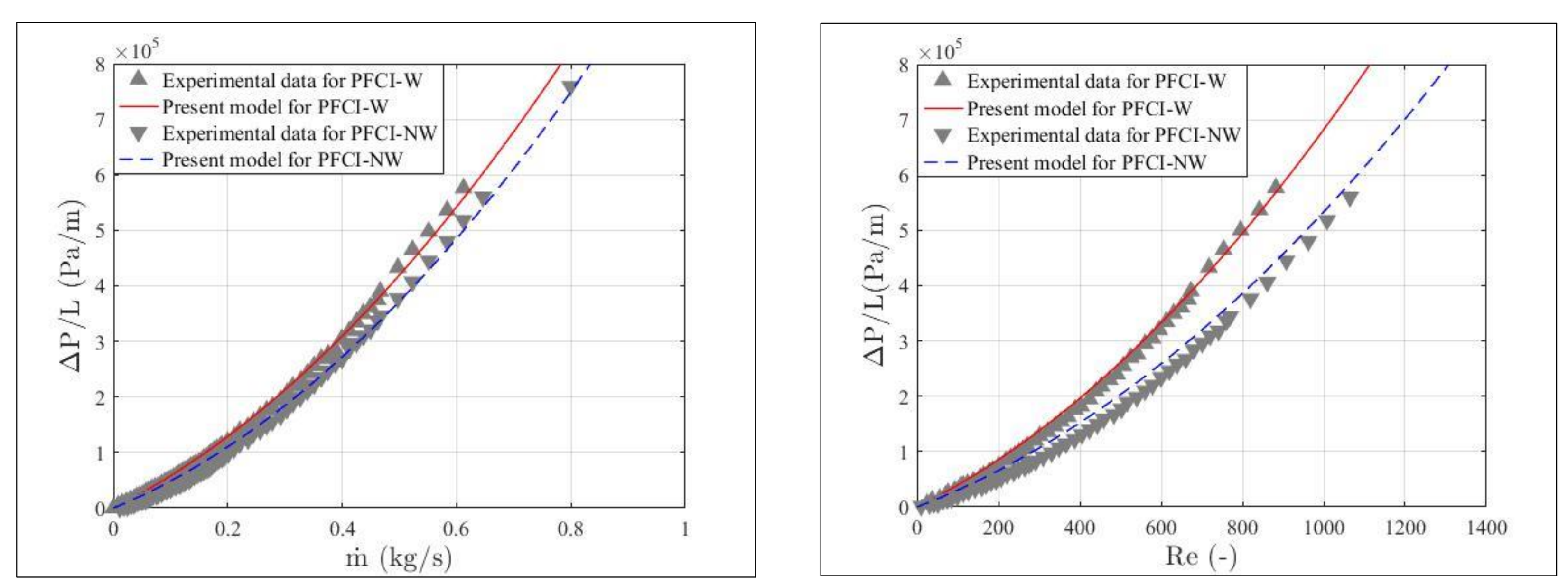

Fig. 3. Pressure drop predictions compare to experiments for PFCI conductor samples.

- The pressure drop predictions of the new model for PFCI-W and PFCI-NW conductor samples are in good agreement with the experimental data.

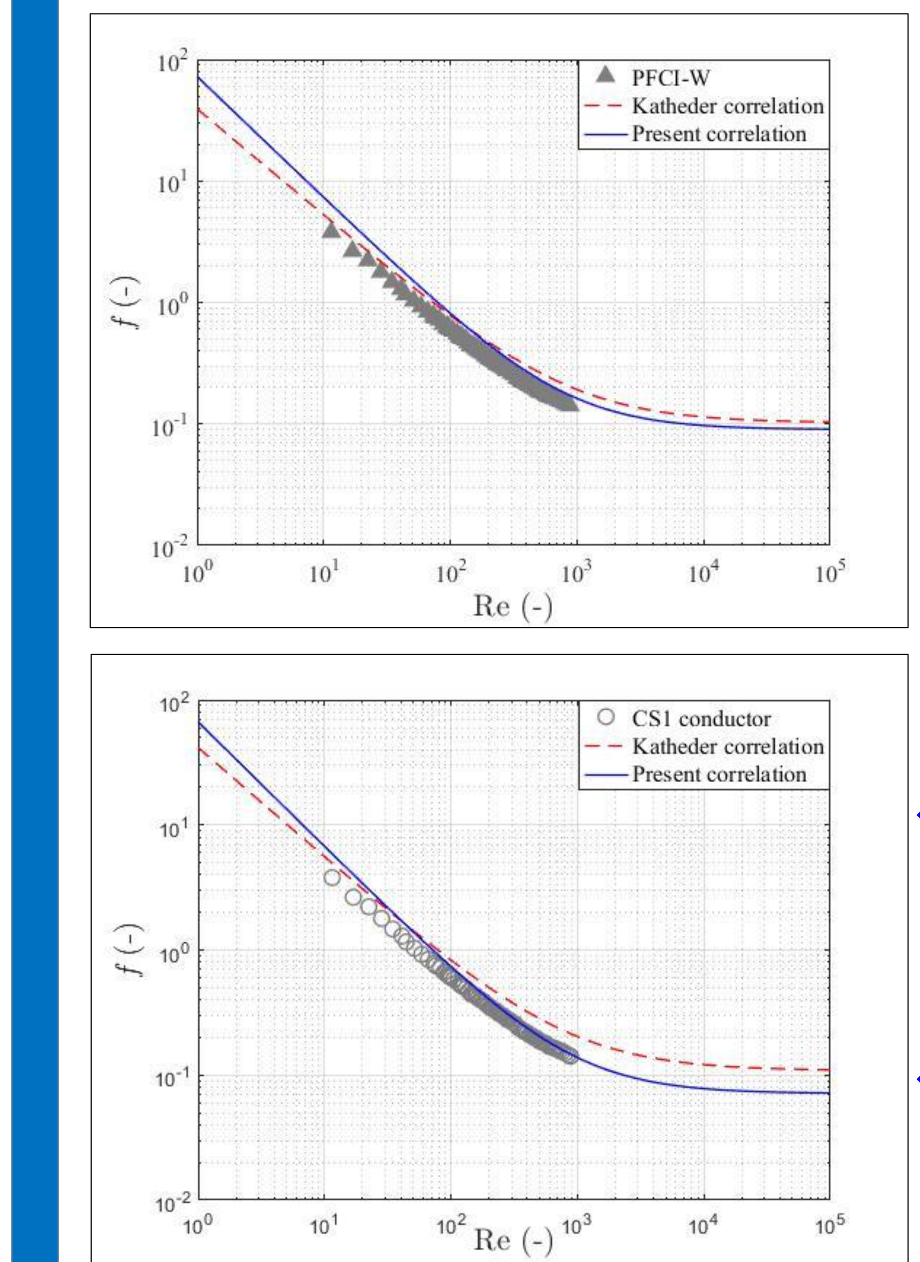

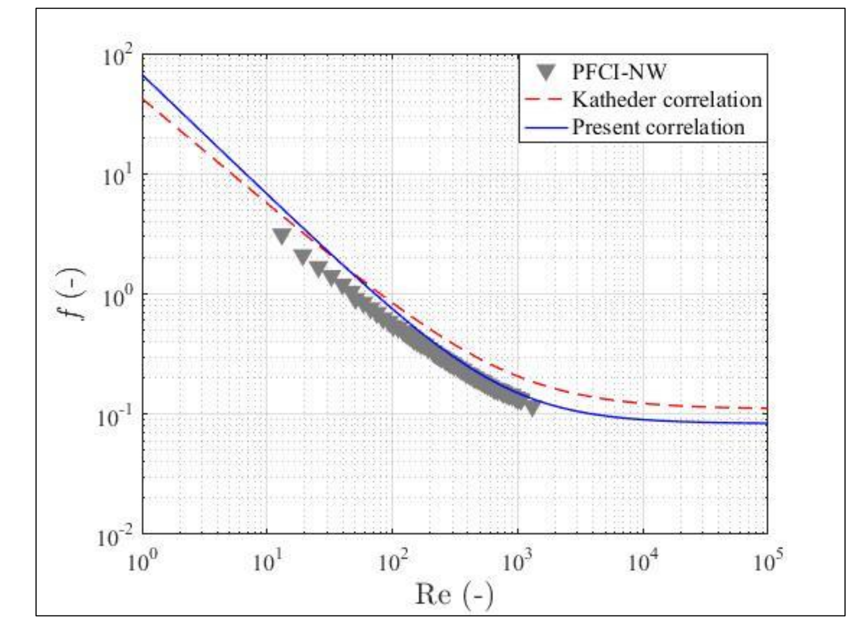

Fig. 4. Comparison of friction factor between the present model predictions with the experimental data.

- The predictions of the new friction factor correlation for PFCI-W, PFCI-NW and CS1 conductors are in good agreement with the experimental data.
- The new friction factor correlation is superior to the Katheder correlation at large Reynolds number.

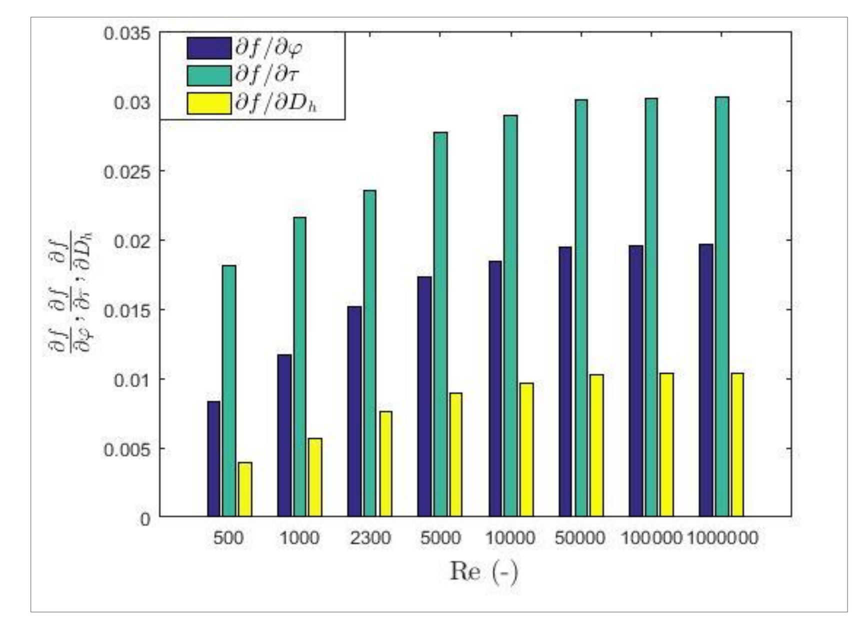

Fig. 5. Effects of void fraction, tortuosity and hydraulic diameter on friction factor at different Reynolds number.

- The main parameters affecting the friction factor are void fraction, tortuosity and hydraulic diameter. For different CICCs, the void fraction has a greater influence than the tortuosity and hydraulic diameter, which explains why the Katheder correlation can be used to predict the friction factor of CICCs.

Conclusions

- An analytical model for predicting the pressure drop of CICCs is developed based on an analogy to porous media.
- An analytical model for predicting the friction factor of CICCs is also derived, the obtained expression is superior to the Katheder correlation at large Reynolds number.
- In the CICCs design, the cabling angle should be decreased, the void fraction should be increased. As the void fraction increases, the hydraulic diameter and the fluid area will also increase, so that the pressure drop will decrease for a given mass flow.